AAPS PharmSciTech, Vol. 10, No. 3, September 2009 (© 2009)
DOI: 10.1208/s12249-009-9265-7

Research Article

The Drug Release Study of Ceftriaxone from Porous Hydroxyapatite Scaffolds

Zeki N. Al-Sokanee,[1,3] Abedl Amer H. Toabi,[1] Mohammed J. Al-assadi,[1] and Erfan A. S. Alassadi[2]

Received 9 January 2009; accepted 15 May 2009; published online 5 June 2009

Abstract. Hydroxyapatite (HAP) is an important biomedical material that is used for grafting osseous defects. It has an excellent bioactivity and biocompatibility properties. To isolate hydroxyapatite, pieces of cleaned cattle's bone were heated at different temperature range from 400°C up to 1,200°C. A reasonable yield of 60.32% *w*/*w* HAP was obtained at temperature range from 1,000°C to 1,200°C. Fourier transform infrared spectra and the thermogravimetric measurement showed a clear removal of organic at 600°C as well as an excellent isolation of HAP from the bones which was achieved at 1,000–1,200°C. This was also confirmed from X-ray diffraction of bone sample heated at 1,200°C. The concentration ions were found to be sodium, potassium, lithium, zinc, copper, iron, calcium, magnesium, and phosphate present in bones within the acceptable limits for its role in the bioactivity property of HAP. Glucose powder was used as a porosifier. Glucose was novel and excellent as porogen where it was completely removed by heating, giving an efficient porosity in the used scaffolds. The results exhibited that the ceftriaxone drug release was increased with increasing the porosity. It was found that a faster, higher, and more regular drug release was obtained from the scaffold with a porosity of 10%.

KEY WORDS: ceftriaxone; drug release; hydroxyapatite.

INTRODUCTION

Hydroxyapatite (HAP) belongs to the group of calcium phosphates, under which ceramic materials with different amounts of calcium and phosphorus were classified. The name apatite was described by the general chemical formula $M_{10}(XO_4)_6 Z_2$ where M could be Ca^{2+}, Ba^{2+}, Sr^{2+}, Pb^{2+}, Mg^{2+}, Zn^{2+}, Si^{2+}, or Na^{+}; X could be P^{5+}, V^{5+}, Cr^{5}, or Mn^{5+}; and Z could be Cl^{-}, F^{-}, or OH^{-} (1).

The term "apatite" was derived from the Greek word "apatao" which means "to deceive." Probably, the structural similarity of different possible mineral compositions was deceiving or misleading to ancient Greek researches. HAP $[Ca_{10}(PO_4)_6(OH)_2]$ was the inorganic component of the natural bone and teeth, but it could be chemically synthesized (2, 3). It is an important material in biology and chemistry. HAP was normally used medically, where HAP and HAP-containing polymer ceramics were important components of the current and the future biomedical materials; also, it has nonmedical applications (4).

Although HAP manufacture is a standard practice in the USA, Europe, and Japan, the cost of this material to non-HAP-manufacturing country or countries with developing economies remains very high, therefore, requiring a cheaper local HAP source (5). Given that bone accounts for about 16–20% of the carcass weight and the current worldwide drive to be more economically efficient in the processing of raw products, achieving added value other than meat uses, such as bone use, is an important priority (6). Considerable efforts were invested to study the effect of the heat treatment on the bone since the calcined bone can be used as osteoreproductive biomaterial for filling osteal defects (7).

Today, HAP biomaterial is clinically widely used in the form of powders, granules, dense and porous blocks, and with various composites (8). This could be attributed to the great biocompatibility and bioactivity properties of HAP, which is probably due to its close chemical similarity with the inorganic components of bone and teeth (9). The delivery of antibiotics using HAP as a drug carrier was studied in the treatment of osteomyelitis (10). Osteomyelitis is a bone infection often caused by bacteria called *Staphylococcus aureus*. *Escherichia coli*, *Enterobacteriaceae* species, anaerobes, and others were also reported. This infection mostly resulted in progressive inflammatory destruction of bone tissue, thereby inhibiting bone regeneration (11). It is clear from literature survey that HAP is a material with admirable characteristics like the biocompatibility and bioactivity. It is available and is a low-cost raw-material-derived substance with multiple applications, mostly medical. In this study, HAP was isolated from cattle bones and supported the ceftriaxone antibiotic on it, evaluating the release characteristics *in vitro*. The effect of the porosity factor on the release efficiency was also studied.

MATERIALS

Acetone, diethyl ether, nitric acid, sodium chloride, potassium chloride, lithium chloride, zinc nitrate hexa

[1] Chemistry Department, College of Science, Basrah University, Basrah, Iraq.
[2] Al-Shafa Hospital, Health Ministry, Basrah, Iraq.
[3] To whom correspondence should be addressed. (e-mail: zekinasser99@yahoo.com)

Table I. The Data of the Thermal Treatment of the Raw Bone

Temperature	Weight before heating (g)	Weight after heating (g)	Yield %	Color of product
400°C	50.4112	37.3597	74.11	Pale orange
500°C	50.3324	34.6136	68.77	Slightly gray
600°C	50.3786	33.4765	66.45	White
700°C	50.3661	32.7782	65.08	White
800°C	50.4153	31.6960	62.87	White
900°C	50.3647	30.7929	61.14	White
1,000°C	50.3952	30.4638	60.41	White
1,100°C	50.3531	30.3629	60.30	White
1,200°C	50.3953	30.3631	60.25	White

hydrates, copper nitrate, ammonium ferrous sulfate, calcium nitrate, magnesium nitrate, potassium dihydrogen orthophosphate, sulfuric acid, ammonium molybdate, stannous chloride, glucose powder, and dibasic sodium phosphate were supplied by B.D.H., H&W Fluka Co., while ceftriaxone was supplied by Ranbaxy Co., India.

METHODS

Bone Sample Preparation

Cattle shoulder bones were collected from local commercial butcheries in Basrah city. The bone samples were thoroughly washed with distilled water to remove the macroscopic adherent impurities, and then cut into small pieces, and treated as described in literature (5). Different weights of the chemically treated bone pieces, which were exactly 50.4112, 50.3324, 50.3786, 50.3661, 50.4153, 50.3647, 50.3952, 50.3531, and 50.3953 g were heated using muffle furnace at the nine different temperatures 400°C, 500°C, 600°C, 700°C, 800°C, 900°C, 1,000°C, 1,100°C, and 1,200°C as shown in Table I, at a heating rate of 10°C/min for 6 h (12).

Porous HAP Scaffolds Preparation

A glucose powder, as porogen, was homogenously mixed with the powdered form of the bone sample heated at 1,200°C to produce glucose–HAP powder mixtures of 2%, 4%, 6%, 8%, and 10% *w*/*w*, each of which contains 1 g of HAP powder. By using a tabulating machine, the powder mixtures were pressed into scaffolds and the average scaffold weight for each percentage was recorded. The composition data for the HAP scaffolds are presented in Table II. The scaffolds were heated in the muffle furnace at 550–600°C for 2 h to get rid of glucose; then, the porous HAP scaffolds were heated at 1,000°C for 6 h to increase the solidification of the scaffolds. After cooling, the average scaffold weight for each percentage was gained and the scaffolds were photographed and then kept in desiccators.

Preparation of Phosphate Buffer Solution

A phosphate buffer of pH 7.4 was prepared by mixing of 0.2 M monobasic sodium phosphate with 405 ml of 0.2 M dibasic sodium phosphate, diluted to a total of 1,000 ml (12).

Ceftriaxone Drug Buffer Solutions

Five identical solutions were prepared by mixing 90 ml of the phosphate buffer solution with 10 ml of the 10% *w*/*v* ceftriaxone solution. The pH of the final solutions was 7.4.

Ceftriaxone Loading on the HAP Different Porosity Scaffolds

The five HAP different porosity scaffolds were immersed in the five ceftriaxone buffered solutions. The containers of the solutions were tightly closed and left for 24 h. After that, the absorbance of ceftriaxone in the five solutions was measured at 240 nm using UV-visible spectrophotometer (13).

Changing the Immersing Solutions

The five different HAP porosity scaffolds were transferred into five 100-ml solutions of a freshly prepared phosphate buffer with pH 7.4.

Follow-up of the Ceftriaxone Release

The magnetic stirrer assembly with an attached hot plate was adopted for the study. The dissolution medium consisted of 100 ml of phosphate buffer (pH 7.4) maintained at 37±1°C by means of a thermoregulated hot plate. The magnetic stirrer was set at a speed of 100 rpm. One-milliliter samples

Table II. The Composition Data for the HAP Scaffolds

Intended porosity	Weight of HAP (g)	Weight of glucose (g)	Total weight of the scaffold (g)
2%	1	0.0204	1.0204
4%	1	0.0416	1.0416
6%	1	0.0638	1.0638
8%	1	0.0869	1.0869
10%	1	0.1111	1.1111

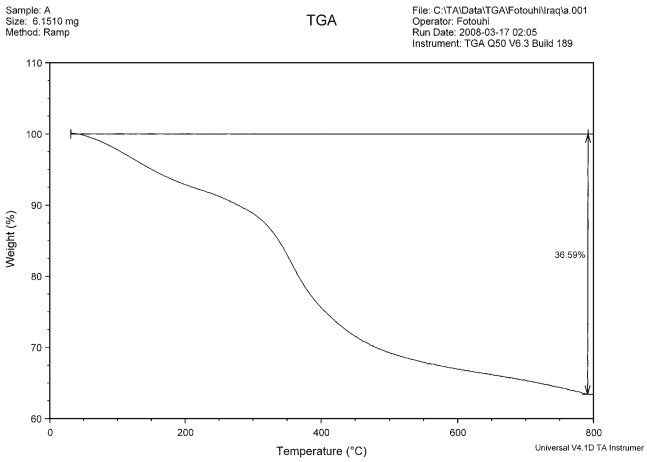

Fig. 1. Thermogram of raw bone

were withdrawn at predetermined time intervals for all the batches. For each sample withdrawn, an equivalent volume of phosphate buffer was added to the dissolution medium to ensure sink condition was maintained throughout.

The release profiles of the ceftriaxone drug from the five different HAP porosity scaffolds was followed for 8 h at a time interval of 15 min in the first 3 h, 30 min in the next 5 h, using UV-visible spectrophotometer. The amount of the ceftriaxone drug released, in milligram, was obtained from the ceftriaxone calibration curve. The drug release was evaluated using the following definition (14):

$$\text{Drug released}(\%) = \frac{\text{Amount of drug released(mg)} \times 100}{\text{Total amount of drug loaded(mg)}}$$

RESULTS AND DISCUSSIONS

The organic components of bones are about 30–35% *w*/*w* and the remaining is inorganic and it is important to remove the unwanted organic components for use as bone repair and regenerative materials. In this study, all the organic impurities were eliminated by heat treatment method in order to get antigenic-free inorganic bone minerals (15). The raw bone pieces subjected to heat treatment at temperature range of 400–1,200°C and the obtained data are shown in Table I. There are two resultant parameters in the heat treatment, the yield and the color of the product. It is obvious that the yield percentage of the heating product is decreased with increasing temperature up to 1,000°C. This could be due to the fact that increasing the temperature could further remove substances that would not be removed at lower temperatures. In addition, it is clear that the yield percentage of the heating products is nearly constant at 1,000°C and above, which leads to the conclusion that most materials other than HAP have been removed.

The nearly constant yield of HAP at the temperature range of 1,000–1,200°C which has a mean value of 60.32% was considered as satisfactory one for the production of this material. Also, the colors of the heating products range from pale orange to slightly gray and finally to white color (12). The pale orange color was characteristic of the 400°C heating product. This color gives an indication that residues of the organic materials were still found with the product. At 500°C, the color was changed into slightly gray, which might be due to the organic impurities that was much reduced at this temperature. This color is replaced by the white color at 600°C and over which gives the indication for removal of all organic components.

Thermogravimetric Analysis

The TG analysis of raw bone was carried out and the thermogram is shown in Fig. 1. There are three ranges of weight loss that can be assigned to the thermogravimetric analysis of the raw bone (16). The thermogram shows an initial weight loss (about 7.1%) up to 200°C which is attributed to water loss. The weight loss between 200°C

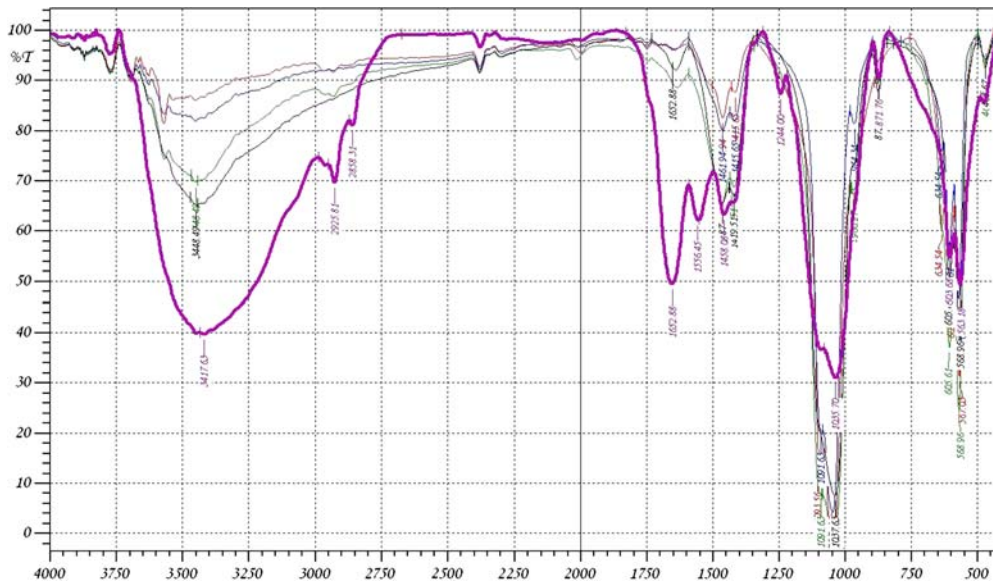

Fig. 2. The FTIR spectra of bone sample (*violet* at room temperature, *black* at 400°C, *green* at 500°C, *blue* at 600°C, *red* at 700°C)

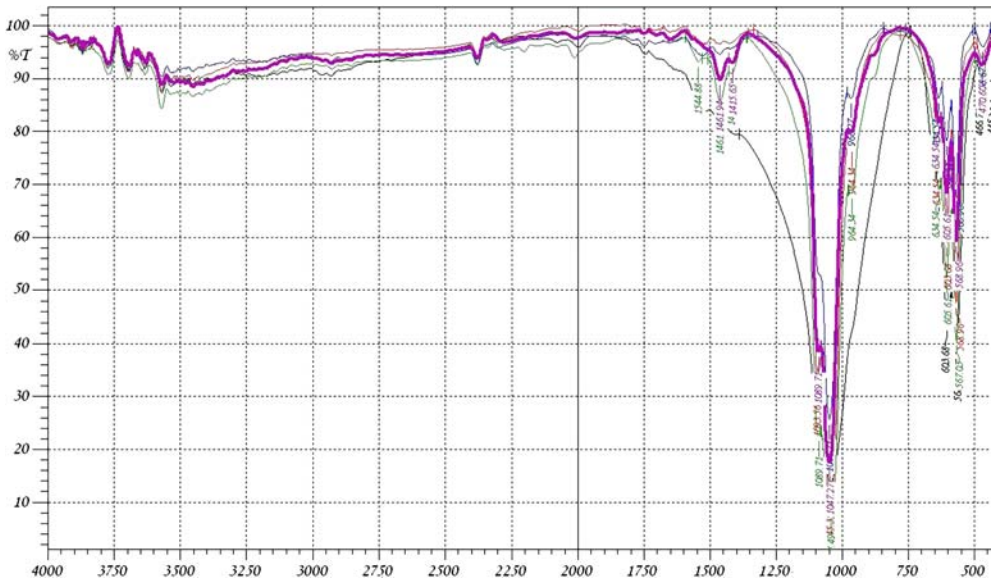

Fig. 3. The FTIR spectra (*violet* at 800,*green* at 900°C, *red* at 1,000°C, *blue* at 1,100°C, *black* at 1,200°C)

and 300°C (about 3%) might be due to mixed water and organics loss. A continuous weight loss (about 22.9%) was observed from 300°C to 600°C due to the decomposition of organic debris (like collagen, fat tissues, and proteins) associated with the bone. At about 600°C, only the mineral phase (calcium phosphate) was left. There was no significant weight loss occurring between 600°C and 800°C, which may suggest that the collagen, fat tissues, and proteins associated with the organic contents of the raw bone were removed at 600°C and above. The small weight loss (about 3.59%) above 600°C is attributed to the decomposition of carbonate present in bone in the form of carbonated apatite (all biological apatites are carbonated). The dissociation of carbonate is reported to occur at temperatures between 600°C and 890°C (12).

Identification of HAP by IR Spectroscopy

The Fourier transform infrared (FTIR) spectra of the raw bone and the heat-treated bones are shown in Figs. 2 and 3. It was found that the IR spectrum of most of the samples shows a major peak at 3,450 cm^{-1} which is due to the –OH group stretching. For the raw bone, the C–H stretching band appears around 2,900 cm^{-1} as an asymmetrical vibration while the symmetrical stretching vibration is shown at about 2,850 cm^{-1}. The strong C=O stretching band can be found at 1,652 cm^{-1} while the amide band presents at 1,550 cm^{-1}. These two peaks are attributed to macromolecules of proteins associated with heat-untreated bone. They are weakened when the bone material was thermally treated at 400°C and disappeared for the bone heated at 600°C and above. The FTIR spectrum of bone heated at 500–1,200°C exhibited the characteristic absorption peaks of HAP (17). The spectra indicate the presence of PO_4^{-3} and OH ions in all of these samples. The bands at 1,035–1,045 and 970–960 cm^{-1} were assigned to the stretching vibration of P=O, while 605 cm^{-1} and 568 cm^{-1} were assigned to its deformation mode (18). Bands at 3,570 cm^{-1} and 634 cm^{-1} were assigned to the vibration motion of the OH ions (19). The OH intensity at 3,450–3,570 cm^{-1} is decreased with increasing the temperature. The decreased intensity up to 600°C is due to loss of water and organics. The decreased intensity above 600°C is due to the breakage of the hydrogen bonding. The OH stretching is not clear at 1,200°C, but the X-ray diffraction of the sample heated at 1,200°C confirms the presence of OH group when compared with the data

Table III. The Increase in Transmittance Percent for CO_3^{-2} with Increasing the Temperature

Temperature	T %
Room temperature	62%
400°C	65%
500°C	66%
600°C	81%
700°C	83%
800°C	85%
900°C	89%
1,000°C	95%
1,100°C	97%
1,200°C	Undetectable

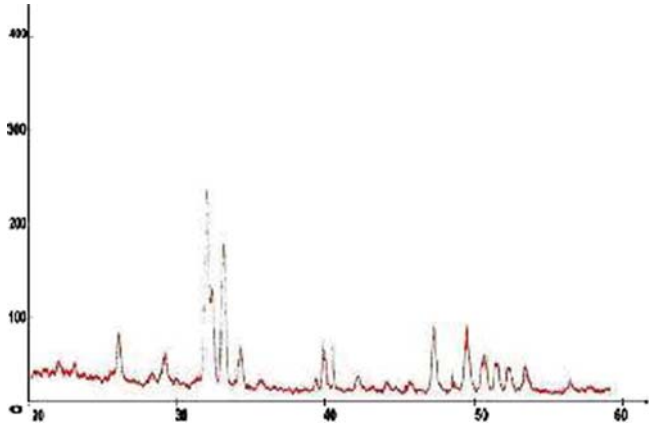

Fig. 4. Diffractogram of bone sample heated at 1,200°C

Table IV. 2θ Values, $d_{2\theta}$ Values, I_{rel} Values Observed for Bone Sample Heated at 1,200°C with the $d_{reference}$ Values

Sequence	2θ	$d_{2\theta}$ (nm)	$d_{reference}$ (nm)	I_{rel}
1	21.8	0.407	0.408	9
2	22.85	0.388	0.489	9
3	25.9	0.343	0.344	26
4	28.25	0.315	0.317	8
5	29	0.307	0.308	18
6	31.85	0.280	0.281	100
7	32.2	0.277	0.278	48
8	33	0.271	0.272	72
9	34.15	0.262	0.263	20
10	35.5	0.252	0.253	6
11	39.3	0.2289	0.2297	8
12	40.1	0.2245	0.2263	32
13	42.1	0.2143	0.2150	8
14	44.1	0.2051	0.2063	6
15	45.4	0.1995	0.2000	8
16	47	0.1931	0.1944	43
17	48.2	0.1885	0.1891	13
18	49.6	0.1835	0.1841	34
19	50.65	0.1800	0.1807	20
20	51.4	0.1775	0.1781	14
21	52.2	0.1750	0.1755	12
22	53.25	0.1718	0.1721	14
23	56.1	0.1637	0.1645	8

obtained from the X-ray results of other workers (20–22). The IR spectra also indicate the absorption peaks of CO_3^{-2} ions around 1,460 cm^{-1} as a symmetrical stretching in all of the used samples (23). The asymmetrical stretching band for CO_3^{-2} can be found at 871 cm^{-1}. The amount of CO_3^{-2} witnessed a small decrease for the bone heated at 500°C as compared to raw bone as shown in Table III, which may be attributed to the existence of organic impurities associated with the bone. The bone samples heated at 600–1,200°C showed a much decreased CO_3^{-2} content because of the high-temperature exposure, which was consistent with our expectation. The intensity of the CO_3^{-2} asymmetrical band at 871 cm^{-1} disappeared at 600°C due to its decreased energy.

IDENTIFICATION OF HAP BY X-RAY DIFFRACTION

The X-ray diffraction was considered as a fingerprint for the compound. The most important parameter in the confirmation of the structure of a compound is the d value, which represents the distance between atomic planes in a crystal. The d values must be consistent for any diffractogram of the same compound. The allowed difference in the 2θ values among the diffractograms of the same compound is 0.3 (24). The X-ray diffraction pattern of the powdered form of the bone sample heated at 1,200°C is shown in Fig. 4. The observed positions of the diffraction lines (2θ and corresponding $d_{2\theta}$) and their relative intensities (I_{rel}) are listed in Table IV. The $d_{2\theta}$ values were calculated according to an equation derivate from Bragg law (25). This is stated below:

$$d(nm) = 0.154/2Sin\theta$$

Where θ represents the angle between the incident X-ray beam and crystal surface layers planes. The relative intensities of the diffraction lines were determined as diffraction line heights relative to the most intense line normalized to the intensity of 100. The $d_{2\theta}$ and I_{rel} values obtained for the bone

Table V. Estimated and Reference Elements Concentrations

Sequence	Element	Estimated element concentration (ppm)	Reference element concentration (ppm)
1	Sodium	975	1,000
2	Potassium	550	570
3	Lithium	15	15. 1
4	Zinc	27.3	28
5	Copper	9.99	9.99
6	Iron	96.24	107
7	Calcium	39,600	39,800
8	Magnesium	640	670
9	Phosphate	56,000	56,773

Fig. 5. Photograph of porous HAP scaffolds

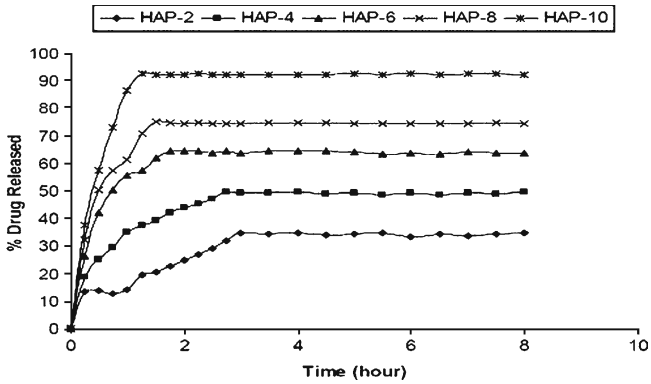

Fig. 7. The *in vitro* release profiles of ceftriaxone from the HAP scaffolds for 32 h. HAP-2: SD±0.32, HAP-4: SD±0.21, HAP-6: SD±0.38, HAP-8: SD±0.18, HAP-10: SD±0.34

sample heated at 1,200°C are almost at full agreement with corresponding reference values reported for HAP (3). These results confirm the formation of HAP; the Bragg peaks in Table V corresponded to the characteristic peaks of HA (JCPDS9-432). The PHA is relatively crystalline, which is characteristically similar to crystallographic geometry of the human bone mineral (26) and matches ionic substituted HAP. However, the overall diffracted peaks of HAP show poor crystallinity compared to that of HAP. There are two possible reasons for the occurrence of low crystallinity: (1) low-temperature processing method and (2) presence of CO_3^{-2} ions associated with the bovine bone.

Quantitative Analysis of Bone Elements

The major constituent elements of the solid skeleton are calcium and phosphate (27). These two elements represent the fundamental elements of the bioapatite. The calcium to phosphorous (Ca/P) ratio is very important for the bioactivity of HAP (6). In addition to the calcium and phosphate, the solid skeleton contains variety of other elements like sodium, potassium, iron, magnesium, copper, and others (28). These elements present in lower quantities than the calcium and phosphate, though they have a vital biofunctionality in the solid skeleton of vertebrates. Flame photometry and phosphomolybdenum blue method were used for the determination of elements in the heat-treated bone sample. Table V shows the concentrations of some major elements found in bone.

Preparation of Porous HAP Scaffolds

Porous HAP scaffolds were made by mixing measurable amounts of glucose powder with 1 g of HAP powder for each intended percent of porosity as given in Table II, pressing the mixture into scaffolds. The glucose was used due to its compressibility, availability, ease of removing, cost, and availability. After heating the scaffolds in the muffle furnace at 550–600°C, it was found that the weight of each porosity percent scaffold was 1 g. This gives an impression that complete removal of glucose was achieved at this temperature. Experimentally, the glucose alone was heated at 550–600°C, where nearly complete removal was achieved in 1 h. The use of glucose as a porogen to induce the required porosity in the HAP scaffolds was novel and very successful, as compared with porogens used by other investigators (29), where the results confirmed that the glucose was good porogen that produced the intended porosity in the HAP scaffolds with the ease of the subsequent complete removal by heating. Figure 5 represents a photograph of the porous HAP scaffolds obtained in our study.

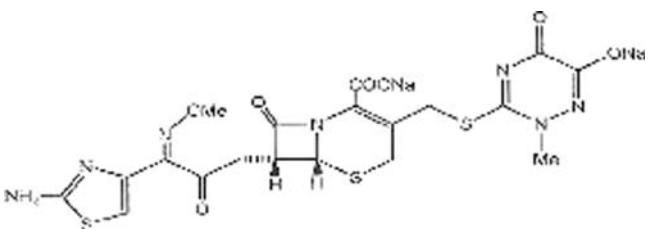

Fig. 6. Structure of ceftriaxone antibiotic

Drug Loading and Release

The drug loading and release profiles were examined under *in vitro* physiological conditions. The HAP scaffolds were loaded with a model drug (i.e., ceftriaxone) which is used in treatment of patients with infectious diseases like osteomyelitis. To define the drug release condition, the effect of scaffold porosity was investigated. The expected mechanism for the drug release from the scaffolds is by diffusion. The structure of ceftriaxone antibiotic is shown in Fig. 6. The amount of drug loaded for each scaffold was determined via the ceftriaxone calibration curve, recording the concentration difference of the release medium before and after loading.

Table VI. Loading and Release Data of Ceftriaxone

Sample	Amount of drug in loading buffer (mg)		Amount of drug loaded (mg)	% loading of drug
	Initial	Final		
HAP-2	1,000	616	384	38.4
HAP-4	1,000	528	472	47.2
HAP-6	1,000	414	586	58.6
HAP-8	1,000	342	658	65.8
HAP-10	1,000	289	711	71.1

The HAP scaffold with a porosity of 10% (HAP-10), the HAP scaffold with a porosity of 8% (HAP-8), the HAP scaffold with a porosity of 6% (HAP-6), the HAP scaffold with a porosity of 4% (HAP-4), and the HAP scaffold with a porosity of 2% (HAP-2) were loaded with 711, 658, 586, 472, and 384 mg, respectively. Then, the weight percentage loading of the drug would be 71.1%, 65.8%, 58.6%, 47.2%, and 38.4% as presented in Table VI. These data indicated that HAP-10 took up a higher amount of the drug than the other scaffolds, which could be attributed to the nature of high porosity.

Figure 7 represent the *in vitro* release profiles of ceftriaxone from the scaffolds. The graphs demonstrate that the amount of drug released from the HAP-10 was higher than the HAP-8, HAP-6, HAP-4, and HAP-2. It is noticed that the increase of the drug amount released from the scaffold reflects the increase in porosity. This is due to fact that the increased porosity would increase the drug loading, as shown from the loading results; also, it increases the fraction of exposed drug molecules in HAP scaffold, leading to increase of the amount of drug released. The above results showed that, in all cases, there is an initial burst release followed by a prolonged release. The initial rapid release is attributed to the initial high difference in drug concentration gradient between the scaffolds and the release medium. This burst release is advantageous for the rapid action of the drug. A 34.78% drug release from HAP-2 was observed within 3 h, 49.65% from HAP-4 within 2.75 h, 64.65% from HAP-6 within 1.75 h, 75.01% from HAP-8 within 1.5 h, and 92.61% from HAP-10 within 1.25 h. The difference in initial burst release from the different scaffolds is also attributed to the porosity factor (29).

It is clear that there is an increase in the regularity of the release profile from the HAP scaffolds with increasing the porosity, with the most regular release coming from HAP-10. This relation is reflected by the decrease in standard deviation values with the increase in porosity; this release regularity is important to achieve nearly a constant level of the drug. This relationship between the regularity and the porosity may be due to the fact that the increase in porosity could increase the motion freedom of the molecules to be regularly carried out of the scaffolds by the solvent. It was found that 34.2% of the drug was released within 5 h from HAP-2 scaffold, whereas 92.32% was released from HAP-10 scaffold within the same period as shown in Fig. 7. This difference in release percentage is due to the porosity difference. The results showed that the HAP-10 release profile is better than the HAP-8, HAP-6, HAP-4, and HAP-2, where it has faster and higher initial release followed by more regular release than all of the others, though the HAP-10 can be used as drug carrier for the delivery of ceftriaxone to skeletal system and would give rapid, effective, and regular action of the drug owing to its adequate porosity and controlled drug release characteristics.

CONCLUSIONS

It can be said according to what previously displayed that HAP, which has a variety of applications mostly medical, can be derived with a reasonable yield by the heat treatment of the mammalian solid skeletons which are very available and nearly useless in the developing countries, thus providing a local cheap source of an important biomedical material. Furthermore, the use of glucose as porosifier for the making of porous HAP scaffolds was novel and successful. It was used for this purpose due to its ease of removing, cost, and availability. Also, the HAP scaffold with a porosity of 10% (HAP-10) has proved itself as a good drug carrier for the delivery of ceftriaxone antibiotic where it results in a rapid (about 1.25 h), high percent (about 92.61%), and more regular release (standard deviation 0.14) in an *in vitro* model.

REFERENCES

1. Shalaby SW, Salz U. Polymers for dental and orthopedics applications. Boca Raton: CRC; 2007. p. 79–80.
2. Chakraborty S, Bag S, Pal S, Mukherjee AK. Structural and microstructural characterization of bioapatite using X-ray powder diffraction and Fourier transform infrared technique. J Appl Cryst. 2006;39:385–90.
3. Markovie M, Fowler BO, Tung MS. Preparation and comprehensive characterization of a calcium hydroxyapatite reference material. J Res Natl Inst Technol. 2004;109:553–68.
4. Morales JG, Burgues JT, Fraile TB, Clemente RR. Precipitation of stoichiometric hydroxyapatite by a continuous method. Cryst Res Technol. 2001;36:15–26.
5. Mucalo MR, Foster DL, Wielage B, Steinhaeuser S, Mucha H, Knichton D, *et al.* Appl Biomat Biomech. 2004;2:96–104.
6. Mucalo MR, Foster DL. A method for avoiding the xanthoproteic-associated discolouration in reprecipitated (nitric-acid-digested) hydroxyapatite prepared from mammalian bone tissue. Croat Chem Acta. 2004;77:509–17.
7. Danilchenko SN, Koropov AV, Protsenko IY, Cleff BS, Sukhadob LF. Thermal behavior of biogenic apatite crystals in bone: an X-ray diffraction study. Cryst Res Technol. 2006;41:268–75.
8. Ferraz MP, Monteiro FJ, Manuel CM. Hydroxyapatite nanoparticles: a review of preparation methodologies. J Appl Biomat Biomecha. 2004;2:74–80.
9. Kannan S, Rocha JH, Ventura JM, Lemos AF, Ferreira JM. Effect of Ca/P ratio of precursors on the formation of different calcium apatitic ceramics—an X-ray diffraction study. Scr Mater. 2005;53:1259–62.
10. Kundu B, Sinha MK, Mitra MK, Basu D. Fabrication and characterization of porous hydroxyapatite ocular implant followed by an *in vivo* study in dogs. Bull Mater Sci. 2004;27 (2):133–40.
11. Nicolau DP, Nie L, Tessier PR, Kourea HP. Prophylaxis of acute osteomyelitis with absorbable ofloxacin-impregnated beads. Antimicrob Agents Chemother. 1998;42:840–2.
12. Ooi CY, Hamdi M, Ramesh S. Properties of hydroxyapatite produced by annealing of bovine bone. Ceram Int. 2007;33:1171–7.
13. Sar TK, Mandal TK, Das SK, Chakraborty AK. Pharmacokinetics of ceftriaxone in healthy and mastitic goats with special reference to its interaction with polyherbal drug (Fibrosin®). Intern J Appl Res Vet Med. 2006;4:142–54.
14. Al-Sokanee ZN. Synthesis and evaluation of new drug supported polymers. M.Sc. Thesis, University of Basrah, Iraq; 2000.
15. Murugan R, Rao KP, Kumar TS. Heat-deproteinated xenogeneic bone from slaughterhouse waste: physico-chemical properties. Bull Mater Sci. 2003;26:523–8.
16. Libera LD. High performance liquid chromatography in the analysis and separation of contractile proteins. Basic Appl Myol. 2001;11(3):115–18.
17. Joschek S, Nies B, Kortz R, Goopferich A. Chemical and physicochemical characterization of porous hydroxyapatite ceramics made of natural bone. Biomaterials. 2000;21:1645–58.
18. Featherstone JD, Pearson S, Geros RZ. An infrared method for quantification of carbonate in carbonated apatites. Caries Res. 1984;18:63–66.
19. Rogers KD, Daniels P. An X-ray diffraction study of the effects of heat treatment on bone mineral microstructure. Biomaterials. 2003;23:2577–85.

20. Danilchenko SN, Moseke C, Cleff BS, Sukhadob LF. X-ray diffraction studies of bone apatite under acid demineralization. Cryst Res Technol. 2004;39(1):71–77.
21. Raynaud S, Champion E, Bernache-assollant D, Laval JP. Determination of calcium/phosphorus atomic ratio of calcium phosphate apatites using X-ray diffractometry. J Am Ceram Soc. 2001;84:359–66.
22. Lutterotti L, Scardi P. Simultaneous structure and size-strain refinement by the Rietveld method. J Appl Cryst. 1990;23:246–52.
23. Jensen SS, Aaboe M, Pinholt EM, Hjørting-Hansen E, Melsen F, Ruyter IE. Tissue reaction and material characteristics of four bone substitutes. Int J Oral Maxillofac Implants. 1996;11:55–66.
24. Chyba B. Measurement and acquisition of X-ray diffractometry spectra. Warsaw: TU Wien; 1995. p. 748.
25. Pardo B, Megademini T, André JM. X-UV synthetic interference mirrors : theoretical approach. Revue Phys Appl. 1988;23:1579–97.
26. Murugan R, Sampath Kumar TS, Ramakrishna S. Scaffolds for bone tissue restoration from biological apatite. Scaffolds for bone tissue trends. Biomater Artif Organs. 2006;20(1):35–9.
27. Peter B, Pioletti DP, Laib S, Bujoli B, Pilet P, Janvier P, *et al*. Calcium phosphate drug delivery system: influence of local zoledronate release on bone implant osteointegration. Bone. 2005;36:52–60.
28. Kargin F, Seyrek K, Bulduk A, Aypak S. Determination of the levels of zinc, copper, calcium, phosphorus and magnesium of Chios ewes in the Aydin region. Turk J Vet Anim Sci. 2004;28:609–2.
29. Murugan R, Ramakrishna S. Porous bovine hydroxyapatite for drug delivery. J Appl Biomat Biomech. 2005;3:93–7.